Polymer Chemistry

ROYAL SOCIETY OF CHEMISTRY

PAPER

View Article Online
View Journal | View Issue

Cite this: *Polym. Chem.*, 2020, **11**, 7533

RAFT dispersion polymerization of benzyl methacrylate in non-polar media using hydrogenated polybutadiene as a steric stabilizer block†

Bastien Darmau,[a] Matthew J. Rymaruk, *[a] Nicholas J. Warren, ‡[a] Robert Bening[b] and Steven P. Armes *[a]

A monohydroxy-capped hydrogenated polybutadiene (PhBD) is converted into a macromolecular chain transfer agent *via* esterification using a carboxylic acid-functionalized trithiocarbonate. ^{1}H NMR and UV spectroscopy studies indicated a mean degree of esterification of at least 95%. The resulting precursor is used for the reversible addition–fragmentation chain transfer (RAFT) dispersion polymerization of benzyl methacrylate (BzMA) in *n*-dodecane at 90 °C. In principle, systematic variation of the mean degree of polymerization (DP) of the insoluble structure-directing PBzMA block should enable the formation of PhBD–PBzMA spheres, worms or vesicles *via* polymerization-induced self-assembly (PISA). In practice, only kinetically-trapped spheres are obtained when targeting DPs of up to 300 at 25% w/w solids. However, increasing the copolymer concentration up to 40% or 45% w/w provides access to well-defined worms or vesicles, respectively. Gel permeation chromatography and ^{1}H NMR spectroscopy studies confirmed relatively narrow molecular weight distributions (M_w/M_n < 1.20) and high final BzMA conversions (≥99%), respectively. These diblock copolymer nano-objects were characterized in terms of their particle size and morphology using TEM and DLS and a phase diagram was constructed. According to rheology studies, the free-standing worm gels that are formed at ambient temperature have a critical gelation concentration of approximately 5.0% w/w.

Received 24th September 2020,
Accepted 6th November 2020

DOI: 10.1039/d0py01371d

rsc.li/polymers

Introduction

Polyethylene and polypropylene are ubiquitous in modern day life.[1] Such polyolefins dominate the global industrial production of synthetic polymers: they are utilized in many applications such as the manufacture of bags, pipes, automotive parts and electrical devices.[2] Their physical properties can be tuned over a wide range depending on their molecular weight, crystallinity and tacticity. In 2018 alone, approximately 62 million tonnes of plastic were produced in Europe, of which nearly 50% was polyethylene and polypropylene.[1]

Since Szwarc's development of living anionic polymerization (LAP)[3,4] there has been considerable interest in the preparation of polyolefin-based block copolymers.[4–8] For example, Hillmyer *et al.* prepared a monohydroxyl-capped polybutadiene (PBD) precursor *via* LAP, with the resulting hydrogenated polybutadiene (PhBD) being used to initiate the LAP of ethylene oxide to afford a series of near-monodisperse amphiphilic diblock copolymers.[9] More recently, reversible addition–fragmentation chain transfer (RAFT) polymerization[10–12] has been used to prepare well-defined polyolefin-based block copolymers. For example, in 2000 De Brouwer *et al.*[13] esterified a monohydroxy-functional hydrogenated PhBD precursor using a carboxylic acid-containing dithiobenzoate chain transfer agent (CTA). The resulting precursor was then used to conduct the alternating copolymerization of styrene with maleic anhydride *via* RAFT solution polymerization in either xylene or butyl acetate. In each case, well-defined diblock copolymers with narrow molecular weight distributions (M_w/M_n < 1.20) were obtained. A similar strategy was adopted by Storey and co-workers, who first polymerized isobutylene *via* living cationic polymerization.[14] The resulting polyisobutylene (PIB) was then end-capped with a hydroxyl group before being esterified with a trithiocarbonate-based

[a]*Dainton Building, Department of Chemistry, The University of Sheffield, Brook Hill, Sheffield, Yorkshire, S3 7HF, UK. E-mail: s.p.armes@sheffield.ac.uk, m.rymaruk@sheffield.ac.uk*
[b]*Kraton Polymers LLC, a subsidiary of Kraton Corporation, Houston, Texas 77084-5015, USA*

†Electronic supplementary information (ESI) available: Beer–Lambert calibration curve for PETTC RAFT agent in dichloromethane, UV GPC chromatograms, tabulated characterization data for all diblock copolymers shown in the phase diagram. Oscillatory strain and frequency sweeps. See DOI: 10.1039/d0py01371d

‡Present address: School of Chemical and Process Engineering, University of Leeds, Woodhouse Lane, Leeds, LS2 9JT, UK.

RAFT agent. Chain extension of this PIB precursor with either methyl methacrylate or styrene resulted in well-defined low-dispersity diblock copolymers, albeit contaminated with a minor fraction of residual PIB precursor.

In addition to the preparation of soluble polyolefin-based diblock copolymers, there has also been considerable interest in the preparation and application of polyolefin-based diblock copolymer *nanoparticles*. For example, Bates and co-workers reported that both PEO–polybutadiene (PEO–PBD) and PEO–PhBD underwent self-assembly in aqueous solution to form a range of copolymer morphologies, including spheres, worms or vesicles.[15,16] The same research group also employed PEO–poly(ethylene-*alt*-propylene) (PEO–PEP) spheres and worms as toughening agents to enhance the fracture resistance of epoxy resins.[17] Similarly, Antonietti and co-workers explored the use of PBD–PEO diblock copolymer micelles as templates for the synthesis of both silica and metal nanoparticles.[18] The same research group also reported that PBD–poly(L-glutamate) diblock copolymers could form vesicles in aqueous solution.[19]

Over the past decade, polymerization-induced self-assembly (PISA) has emerged as a versatile synthetic tool that enables diblock copolymers to be synthesized and self-assembled in a single step.[20–22] In PISA, a homopolymer (A) is dissolved in a good solvent. A second polymer (B), which is selected to be insoluble in this solvent, is then grown from one end of this soluble precursor. As the second-stage polymerization proceeds, the resulting AB diblock copolymers form sterically-stabilized nanoparticles (a.k.a. micelles) with the A block acting as the steric stabilizer and the B block being located within the nanoparticle cores. A wide range of PISA formulations have been developed using styrene,[23–25] methacrylics,[26–28] acrylics[29–31] and acrylamides,[32,33] while the continuous phase can be water,[27,34] alcohols,[23,35,36] alkanes,[37–40] silicones,[41,42] haloalkanes,[43] supercritical CO_2 [44] or ionic liquids.[45] PISA is usually highly efficient and enables functional diblock copolymer nano-objects to be conveniently prepared in the form of concentrated dispersions. Very recently, examples of LAP-mediated PISA have been reported in non-polar media.[46,47] However, most of the literature examples of PISA are based on RAFT polymerization.[10,11,48] No doubt this is because such radical-based chemistry is particularly tolerant of monomer functionality and, unlike LAP, does not require the rigorous exclusion of protic impurities such as water.

Herein we report the first example of the preparation of polyolefin-stabilized diblock copolymer nano-objects *via* RAFT-mediated PISA. More specifically, a monohydroxy-capped hydrogenated polybutadiene (PhBD) precursor is esterified using a carboxylic acid-based RAFT agent (see Scheme 1). The resulting trithiocarbonate-capped PhBD precursor is then chain-extended *via* RAFT dispersion polymerization of benzyl methacrylate (BzMA) in *n*-dodecane (see Scheme 1). The target DP of the PBzMA core-forming block is then systematically increased to produce the full range of diblock copolymer nano-objects (spheres, worms or vesicles) and a phase diagram is constructed to facilitate reproducible targeting of such copolymer morphologies. At a copolymer concentration of 25% w/w, only spherical micelles are accessible. Interestingly, the synthesis of worms or vesicles, requires copolymer concentrations of 40–45% w/w. As far as we are aware, this is the first report of the PISA synthesis of either worms or vesicles at such high copolymer concentrations in non-polar media.

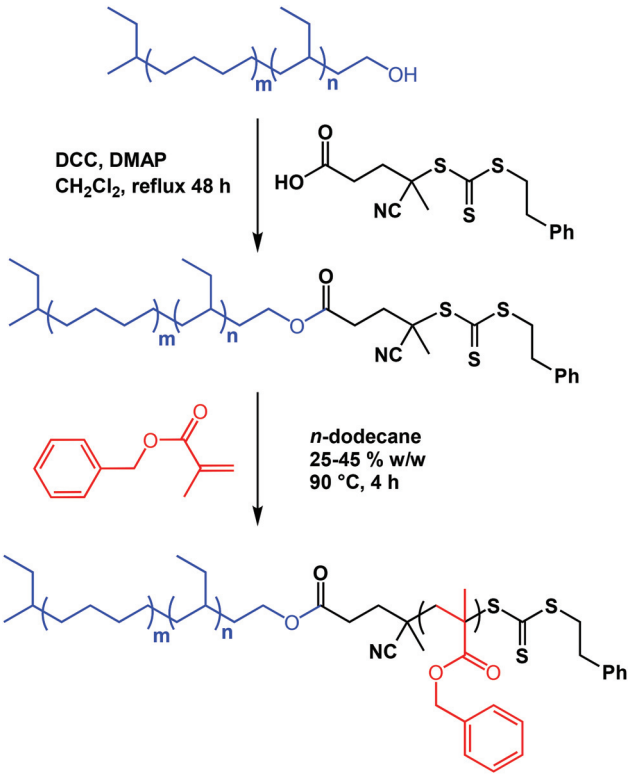

Scheme 1 Esterification of the monohydroxy-functional hydrogenated polybutadiene (DP = 80, *m* = 61 mol%, *n* = 39 mol%) precursor with PETTC, followed by RAFT dispersion polymerization of benzyl methacrylate in *n*-dodecane at 90 °C using the resulting trithiocarbonate-based macromolecular RAFT agent.

Experimental section

Materials

Monohydroxy-capped hydrogenated polybutadiene (M_n = 4500 g mol^{-1}, $Đ$ = 1.09, 61 mol% 1,4-polybutadiene and 39 mol% 1,2-polybutadiene) was kindly donated by Kraton Polymers LLC. (Houston, USA) and was used as received. Benzyl methacrylate, *N*,*N*′-dicyclohexylcarbodiimide (DCC), 4-dimethylaminopyridine (DMAP), dichloromethane, *n*-dodecane, methanol, THF, butylated hydroxytoluene (BHT) and triethylamine were purchased from Sigma Aldrich (UK). Trigonox 21S initiator was purchased from AkzoNobel (The Netherlands). $CDCl_3$ and CD_2Cl_2 were purchased from Goss Scientific (UK).

Methods

Synthesis of the trithiocarbonate-capped hydrogenated polybutadiene precursor. Monohydroxy-capped hydrogenated poly-

butadiene (PhBD; 9.00 g, 2.00 mmol), PETTC RAFT agent (1.36 g, 4.00 mmol) were weighed out into a round-bottomed flask containing a magnetic stirrer bar and dried in a vacuum oven overnight. The flask was equipped with a reflux condenser, evacuated under vacuum and refilled with nitrogen gas. Anhydrous dichloromethane (50 mL) was then added *via* syringe, along with DMAP (49.0 mg, 0.40 mmol, dissolved in 1.0 mL anhydrous dichloromethane prior to addition). The resulting mixture was cooled to 0 °C for 30 min by immersing the flask in an ice bath, before DCC (1.0 g, 5.0 mmol, dissolved in 5.0 mL anhydrous dichloromethane prior to addition) was added dropwise over 20 min. The reaction mixture was then maintained at 0 °C for 60 min before being heated to reflux for 40 h. The reaction mixture was cooled, placed in a freezer overnight, and filtered to remove the dicyclohexylurea precipitate. Finally, dichloromethane was removed from the crude reaction mixture under reduced pressure, prior to purification by precipitation into a ten-fold excess of methanol (three times). ^{1}H NMR spectroscopy studies indicated that 95% of the terminal hydroxy groups had been esterified, (the integrated proton signals assigned to the PhBD backbone were compared to the integrated signal assigned to the five aromatic protons associated with the phenyl end-group on the PETTC RAFT agent. UV spectroscopy studies conducted in dichloromethane indicated a degree of esterification of 97%.

Synthesis of $PhBD_{80}$–PBzMA vesicles in *n*-dodecane by RAFT dispersion polymerization of BzMA. A typical synthesis of $PhBD_{80}$–$PBzMA_{300}$ vesicles at 40% w/w in *n*-dodecane was conducted as follows: PhBD RAFT agent (0.10 g, 23.1 μmol), BzMA (1.15 g, 6.50 mmol, target DP = 300 assuming a mean degree of esterification of 95% for this $PhBD_{80}$ precursor) and *n*-dodecane (1.87 g) were weighed into a 10 mL glass vial equipped with a magnetic stirrer. T21s initiator (1.0 mg, 4.63 μmol, [$PhBD_{80}$]/[T21s] molar ratio = 5.0; 11 μL of a 10% v/v solution in *n*-dodecane) was added to this solution at 20 °C. The resulting mixture was then purged with nitrogen, sealed, and placed in a pre-heated oil bath set at 90 °C for 5 h. After cooling to 25 °C, the final dispersion was obtained as a milky-white paste. ^{1}H NMR spectroscopy studies ($CDCl_3$) confirmed a BzMA conversion of 98%, and THF GPC analysis indicated an M_n of 49 600 g mol^{-1} and an M_w/M_n of 1.20. To obtain either spheres or worms, the mass of $PhBD_{80}$ macro-CTA and T21s initiator was held constant, and the mass of BzMA and *n*-dodecane was varied (see the ESI† for further experimental details).

Characterization

^{1}H NMR spectroscopy. ^{1}H NMR spectra were recorded in either CD_2Cl_2 or $CDCl_3$ using a Bruker AV1-400 MHz spectrometer. Typically, 64 scans were averaged per spectrum.

Gel permeation chromatography. Molecular weight distributions were determined using a GPC set-up operating at 30 °C that comprised two Polymer Laboratories PL gel 5 μm Mixed C columns, a LC20AD ramped isocratic pump, THF eluent and a WellChrom K-2301 refractive index detector operating at 950 ± 30 nm. The mobile phase contained 2.0% v/v triethylamine and 0.05% w/v 3,5-di-*tert*-4-butylhydroxytoluene (BHT); the flow rate was 1.0 ml min^{-1}. A series of ten near-monodisperse poly(methyl methacrylate) standards (M_n = 1280 to 330 000 g mol^{-1}) were used for calibration. Chromatograms were analyzed using Varian Cirrus GPC software.

Dynamic light scattering. Dynamic light scattering (DLS) studies were performed using a Zetasizer Nano-ZS instrument (Malvern Instruments, UK) at 25 °C at a fixed scattering angle of 173°. Copolymer dispersions were diluted in *n*-dodecane to a final concentration of 0.10% w/w. The intensity-average diameter and polydispersity (PDI) of the diblock copolymer nano-objects were calculated by cumulants analysis of the experimental correlation function using Dispersion Technology Software version 6.20. Data were averaged over three consecutive measurements, with each measurement comprising ten runs and each run being of thirty seconds duration.

Transmission electron microscopy. Transmission electron microscopy (TEM) studies were conducted using a FEI Tecnai G2 spirit instrument operating at 80 kV and equipped with a Gatan 1k CCD camera. Copper TEM grids were surface-coated in-house to yield a thin film of amorphous carbon. The grids were then loaded with dilute copolymer dispersions (0.20% w/w). Prior to imaging, each grid was exposed to ruthenium(IV) vapour for 7 min at ambient temperature in order to achieve sufficient contrast. The ruthenium oxide stain was prepared by adding ruthenium(II) oxide (0.30 g) to water (50 g), to form a slurry. Then sodium periodate (2.0 g) was added to the stirred solution and a yellow solution of ruthenium(IV) oxide was formed within 1 min at 20 °C.

UV-visible absorption spectroscopy. UV–visible absorption spectra were recorded between 200 and 800 nm using a PC-controlled UV-1800 spectrophotometer at 25 °C and a 1 cm path length quartz cell. A Beer–Lambert calibration curve was constructed using a series of twelve PETTC solutions in dichloromethane with the PETTC concentration ranging from 1.2×10^{-5} mol dm^{-3} to 1.0×10^{-4} mol dm^{-3}. The absorption maximum at 298 nm assigned to the trithiocarbonate group was used to construct this calibration plot. The mean DP of the PhBD–TTC precursor was determined using the molar extinction coefficient of 10 153 ± 220 mol^{-1} dm^3 cm^{-1} calculated for the PETTC RAFT agent.

Results and discussion

The monohydroxy-capped PhBD (M_n = 4500 g mol^{-1}, $Đ$ = 1.09) was prepared *via* living anionic polymerization of butadiene initiated with *sec*-butyllithium at 26 °C in 90 : 10 w/w anhydrous cyclohexane/diethyl ether; the reaction temperature increased to approximately 40 °C owing to the exothermic nature of the polymerization. A 20 mol% excess of ethylene oxide was added, resulting in the addition of a single unit of ethylene oxide at the end of every polymer chain (degree of ethoxylation >99%).[9] Diethyl ether was used as a co-solvent during polymerization in order to increase the 1,2 content of

the polybutadiene precursor.[49] This protocol was adopted because hydrogenated polybutadienes with lower vinyl contents are known to be prone to crystallization, which we wished to avoid in the present study. Exhaustive hydrogenation of the unsaturated groups was accomplished using a nickel/aluminium catalyst prepared by the reaction of nickel 2-ethylhexanoate with triethylaluminium. This precursor was then esterified using a carboxylic acid-based RAFT agent PETTC using *via* DCC/DMAP coupling chemistry (Scheme 1) to produce the desired macromolecular RAFT agent.

The resulting trithiocarbonate-based PhBD RAFT agent was characterized using UV GPC, ^{1}H NMR spectroscopy and UV spectroscopy. Firstly, UV GPC studies (UV detector wavelength tuned to 298 nm) confirmed that all the unreacted PETTC RAFT agent had been removed from the purified polyolefin-based RAFT agent (see Fig. S1†). ^{1}H NMR studies indicated a mean degree of esterification of 95% by comparing the signals assigned to the polyolefin backbone at 0.7–1.7 ppm with the five aromatic protons associated with the organosulfur-based RAFT end-group at 7.3 ppm (see Fig. 1). UV spectroscopy was used to construct a linear Beer–Lambert calibration curve (see Fig. S2†) at a maximum wavelength of 298 nm (owing to a π–π^* transition) by utilizing a series of PETTC stock solutions of known concentration. The mean degree of esterification of the polyolefin-based RAFT agent was then determined by end-group analysis as follows. First, a known concentration of this precursor was analyzed to determine its absorbance at 298 nm. Then the theoretical absorbance expected for this concentration was calculated using the molar extinction coefficient determined for PETTC. Thus, the mean degree of esterification was calculated to be 97% by dividing the first absorbance by the second absorbance. In this approach, it is assumed that the PhBD RAFT agent and PETTC possess the same molar absorption coefficient. This is a reasonable approximation because the absorption maximum observed for each species is at 298 nm. Moreover, this mean degree of esterification is in good agreement with that estimated by ^{1}H NMR spectroscopy (see Fig. 1), with UV spectroscopy expected to offer significantly greater sensitivity. It is perhaps noteworthy that the caveats noted by Laschewsky and co-workers when using UV spectroscopy to determine mean degrees of polymerization arose from subtle differences in chemical structure between the small molecule RAFT agent and the RAFT-synthesized homopolymers.[50] Such experimental errors are not incurred in the present case because there is no change in the nature of the substituents on the trithiocarbonate group. Indeed, several research groups have reported using UV spectroscopy to determine the degree of esterification (or amidation) for various macromolecular RAFT agents.[41,51–53]

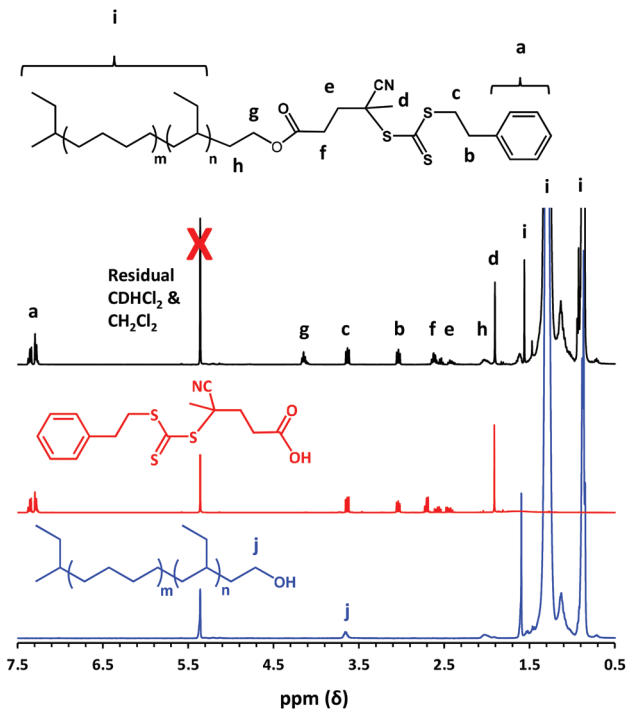

Fig. 1 ^{1}H NMR spectra recorded in CD_2Cl_2 for the monohydroxy-functional PhBD precursor (blue spectrum), the PETTC RAFT agent (red spectrum) and the trithiocarbonate-capped PhBD RAFT agent (black spectrum). The overall PhBD DP is 80 (m = 61 mol%, n = 39 mol%).

Next, the PhBD RAFT agent was employed as the steric stabilizer block for the RAFT dispersion polymerization of BzMA at 90 °C in *n*-dodecane at a copolymer concentration of 25% w/w. A kinetic study was conducted when targeting a PBzMA DP of 200, with aliquots being removed from the polymerizing mixture at regular intervals prior to analysis by ^{1}H NMR spectroscopy (see Fig. 2a). A five-fold rate enhancement was observed after 90 min, which coincided with the onset of turbidity for the polymerizing solution. This effect has been observed in many PISA formulations and is attributed to micellar nucleation.[54] At this point, unreacted BzMA monomer enters the micelle cores which leads to a relatively high local concentration; the ensuing rate acceleration enables 98% BzMA conversion to be achieved within 4 h. GPC analysis of quenched aliquots extracted from the polymerizing solution (Fig. 2b) indicated a linear evolution of M_n with respect to conversion and dispersities remained below 1.20, as expected for a well-controlled RAFT polymerization.[11,55] Selected chromatograms recorded during these kinetic studies are shown in Fig. 3. Inspecting these data, there appears to be significant contamination of the diblock copolymer chains by unreacted PhBD RAFT agent for BzMA conversions at or below 20%. However, this species is gradually consumed as the RAFT dispersion polymerization of BzMA progresses, and its presence is negligible above 80% BzMA conversion. Interestingly, strikingly similar behavior was also reported by De Brouwer *et al.* when using a dithiobenzoate-capped PhBD RAFT agent to conduct the RAFT the alternating copolymerization of styrene with maleic anhydride.[13] One plausible explanation for such slow reinitiation is a relatively low transfer constant for the polyolefin-based RAFT agent.[13] Nevertheless, this problem does not prevent the eventual formation of relatively well-defined diblock copolymer chains (M_w/M_n < 1.20). The weak

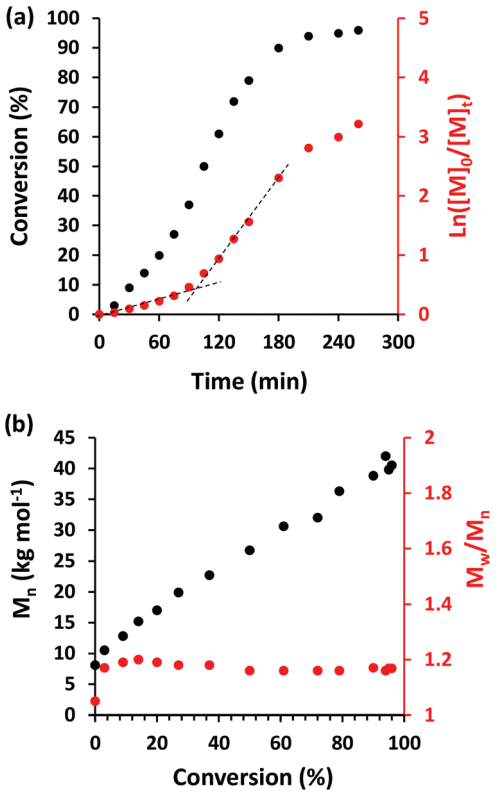

Fig. 2 (a) Conversion *vs.* time (black data) obtained by *ex situ* ^{1}H NMR spectroscopy studies of the RAFT dispersion polymerization of BzMA in *n*-dodecane at 90 C using a PhBD RAFT agent as a steric stabilizer. Conditions: the copolymer concentration was 25% w/w and the PBzMA target DP was 300. The corresponding semi-logarithmic plot is also shown (red data). (b) GPC molecular weight data, expressed relative to a series of poly(methyl methacrylate) calibration standards, obtained for the samples shown in (a). M_n and M_w/M_n data are shown in black and red, respectively.

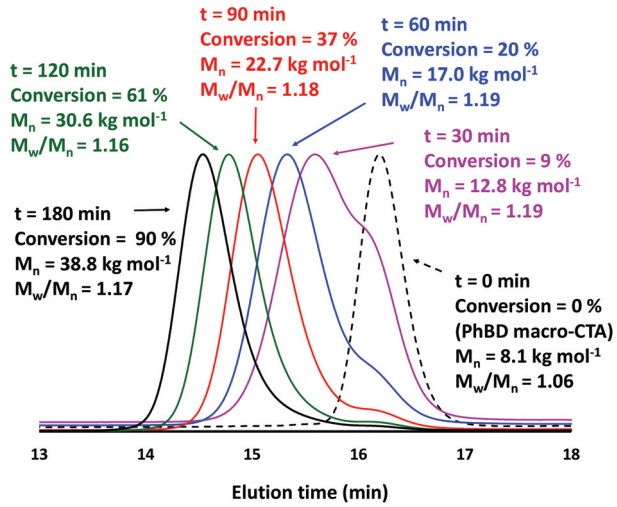

Fig. 3 THF GPC curves (refractive index detector; calibrated using a series of near-monodisperse poly(methyl methacrylate) standards) recorded during the RAFT dispersion polymerization of BzMA in *n*-dodecane at 90 °C. Conditions: target copolymer concentration = 25% w/w, target PBzMA DP = 200 and [PhBD macro-CTA]/[T21s] molar ratio = 5.0.

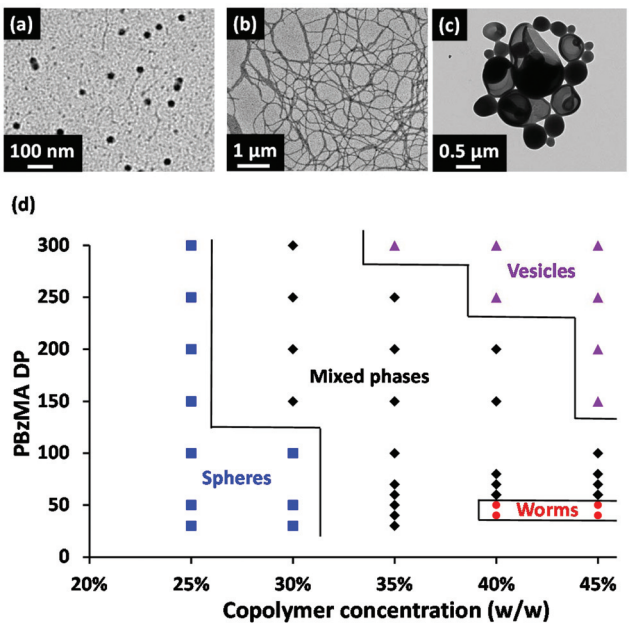

Fig. 4 Representative TEM images recorded for (a) $PhBD_{80}$–$PBzMA_{100}$ spheres prepared at 30% w/w, (b) $PhBD_{80}$–$PBzMA_{40}$ worms prepared at 45% w/w and (c) $PhBD_{80}$–$PBzMA_{300}$ vesicles prepared at 45% w/w. (d) Representative phase diagram for this PISA formulation, with each copolymer morphology being assigned on the basis of TEM analysis.

low molecular weight shoulder still remaining above 80% BzMA conversion is most likely the result of either unreacted PhBD macro-CTA or unesterified PhBD precursor.

Having established pseudo-living character for the RAFT dispersion polymerization of BzMA using this new polyolefin-based RAFT agent, a series of further PISA syntheses were conducted in which the target PBzMA DP and the copolymer concentration were systematically varied, see Table S1.†

The resulting copolymer morphologies were assigned by TEM studies, which enabled the construction of a detailed phase diagram (see Fig. 4). For most literature examples of RAFT dispersion polymerization, targeting copolymer concentrations above 20% w/w is usually sufficient to enable the reproducible synthesis of spheres, worms or vesicles, provided that the steric stabilizer block is not too long.[40,42,56] Thus, we were surprised to discover that only kinetically-trapped spheres could be obtained at 25% w/w copolymer concentration for the current PISA formulation, despite targeting PBzMA DPs of up to 300. At 30% w/w copolymer concentration, spheres were produced for PBzMA DPs of 100 or below, whereas mixed phases were obtained for PBzMA target DPs above 100.

This observation encouraged us to explore further syntheses at even higher copolymer concentrations. Fortunately, this strategy provided access to the full range of copolymer morphologies: highly anisotropic worms were obtained at PBzMA

DPs of 40 and 50 when targeting 40–45% w/w solids, while polydisperse vesicles were obtained at a PBzMA DP of 300 when targeting 35% w/w solids, and at PBzMA DPs of 150–300 when targeting 45% w/w solids.

To assess the evolution of molecular weight when varying the DP of the PBzMA block, a series of diblock copolymers were analyzed *via* THF GPC (see Table S1†). Selected chromatograms obtained for diblock copolymers prepared at 45% w/w are shown in Fig. 5, with the GPC curve obtained for the PhBD precursor included as a reference. There is a systematic shift to shorter elution time (higher molecular weight) as the PBzMA DP is increased from 40 to 300. Relatively high blocking efficiencies are observed in each case, but a small low molecular weight shoulder is also observed that clearly corresponds to the PhBD precursor. In principle, this may indicate non-esterified monohydroxyl-capped $PhBD_{80}$ impurity, but it is also possible that the trithiocarbonate-capped $PhBD_{80}$ precursor suffers from relatively slow initiation. Therefore, this signal could be the result of unesterified $PhBD_{80}$ starting material, uninitiated trithiocarbonate-capped $PhBD_{80}$, or some combination of the two. UV GPC analysis provides a convenient way of ruling out the first of these three possibilities: if the lower molecular weight shoulder is caused solely by unesterified $PhBD_{80}$, it should be absent from the UV GPC curve. Inspecting Fig. S3,† the low molecular weight shoulder is clearly visible in this chromatogram. Thus this feature is assigned, at least in part, to some fraction of as-yet-unreacted $PhBD_{80}$ macro-CTA. However, the presence of residual unesterified PhBD cannot be excluded. Nevertheless, M_n increased linearly with the target PBzMA DP (see Fig. S4†) and dispersities remained below 1.25, as expected for a well-controlled RAFT polymerization.

When targeting PBzMA DPs of up to 300, only kinetically-trapped PhBD–PBzMA spheres were obtained for PISA syntheses conducted at 25% w/w solids. Even at 30% w/w solids, only spheres were obtained for PBzMA DPs of up to 100. DLS was used to assess the effect of varying the PBzMA DP on the *z*-average sphere diameter, see Fig. 6. This double logarithmic plot exhibits a reasonably linear relationship, indicating that the mean sphere diameter can be systematically adjusted between 30 nm and 80 nm simply by varying the DP of the core-forming PBzMA block.

Finally, the $PhBD_{80}$–$PBzMA_{40}$ worm gels were analyzed by rheology to assess their physical properties. First, a large-scale batch (~10 g) of $PhBD_{80}$–$PBzMA_{40}$ worms was prepared in *n*-dodecane. Then portions of this gel were removed and diluted with *n*-dodecane to produce a series of copolymer dispersions with concentrations ranging between 5% w/w and 30% w/w. According to the tube inversion test, free-standing worm gels were obtained at 8% w/w or above, whereas $PhBD_{80}$–$PBzMA_{40}$ worms at 5% w/w or 6% w/w in *n*-dodecane formed a viscous fluid that flowed under gravity. These copolymer dispersions were then analyzed by oscillatory rheology. In each case, a frequency sweep was performed at a constant applied strain of 1.0%, followed by a strain sweep at a fixed frequency of 1.0 rad s^{-1} (see Fig. S5 and S6†). At 40% w/w, $PhBD_{80}$–$PBzMA_{40}$ worms clearly form strong gels, as indicated by the much greater magnitude of G' (24 600 Pa) than G'' (1600 Pa). In the amplitude sweep, G' and G'' are independent of the applied strain up to 1.0%, which indicates the linear viscoelastic regime. At strains above 1.0%, G'' is less than G'. This indicates the yield point, which is associated with loss of the percolating worm network. Both G' and G'' are approximately independent of the applied frequency within the linear viscoelastic regime, which is characteristic of solid-like behavior. Similar behavior was observed for $PhBD_{80}$–$PBzMA_{40}$ worms

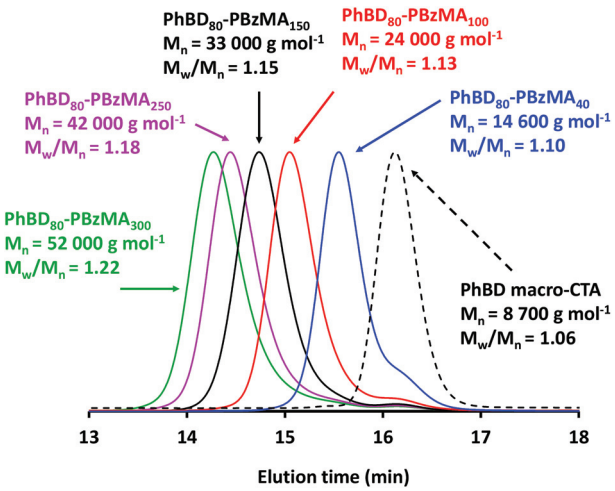

Fig. 5 GPC traces obtained using a refractive detector (THF eluent, calibrated against PMMA standards) for the trithiocarbonate-capped $PhBD_{80}$ precursor (black dashed curve) and a series of five $PhBD_{80}$–$PBzMA_x$ diblock copolymers (see blue, red, black, purple and green curves) prepared by the RAFT dispersion polymerization of BzMA at 45% w/w solids in *n*-dodecane.

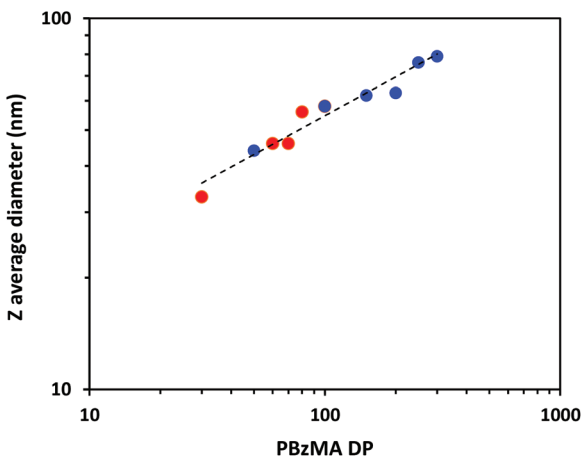

Fig. 6 Effect of varying the DP of the core-forming PBzMA block (*x*) on the *z*-average diameter of $PhBD_{80}$–$PBzMA_x$ spheres in *n*-dodecane, as determined by DLS. The blue circles represent spheres prepared at 25% w/w, whereas the red circles represent spheres prepared at 30% w/w. All copolymer dispersions were diluted to 0.20% w/w in *n*-dodecane prior to DLS analysis.

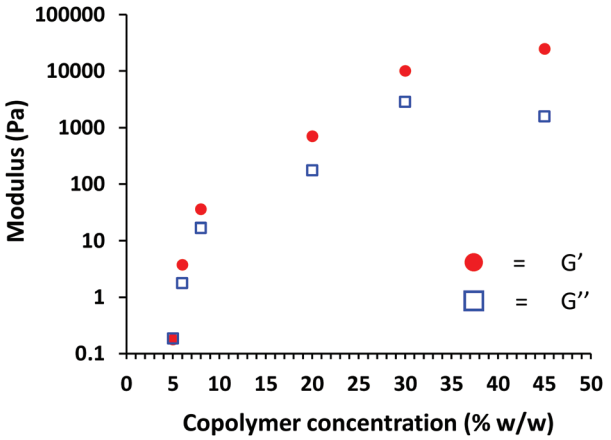

Fig. 7 Elastic (G') and viscous (G'') moduli recorded for $PhBD_{80}$–$PBzMA_{40}$ diblock copolymer worms over a range of copolymer concentrations in *n*-dodecane at an applied strain of 1.0% and an angular frequency of 1.0 rad s^{-1}. The worms were prepared at 40% w/w solids and then diluted to produce a series of lower copolymer concentrations.

between 30% w/w and 6% w/w, albeit with a systematic reduction in G' and G'' being observed at lower copolymer concentrations. However, G' falls below G'' at 5% w/w, indicating that this copolymer concentration corresponds to a viscous fluid. Fig. 7 shows both G' and G'' as a function of copolymer concentration. When G' exceeds G'', the dispersion is deemed to be a gel, whereas when G' is less than G'', the dispersion is considered to be a liquid. Thus, the CGC of these $PhBD_{80}$–$PBzMA_{40}$ worms is estimated to be 5% w/w, which is consistent with CGC values reported for other diblock copolymer worms prepared in non-polar media.[42,56]

Conclusions

A polyolefin-based RAFT agent was prepared *via* esterification of a monohydroxy-functional PhBD precursor using a carboxylic acid-functionalized RAFT agent. ^{1}H NMR and UV spectroscopy studies indicated a mean degree of esterification of at least 95% while UV GPC indicated efficient removal of the unreacted carboxylic acid-based RAFT agent *via* precipitation into excess methanol. The RAFT dispersion polymerization of BzMA in *n*-dodecane was then examined using this polyolefin-based RAFT agent as the steric stabilizer block. ^{1}H NMR studies indicated a five-fold increase in the rate of BzMA polymerization after 90 min, which was attributed to the onset of micellar nucleation. This rate acceleration enabled essentially full conversion to be achieved within 4 h at 90 °C. However, GPC studies indicated relatively slow initiation, with a significant fraction of unreacted polyolefin-based RAFT agent being observed up to 60% BzMA conversion. Nevertheless, this precursor was gradually consumed as the BzMA polymerization progressed, yielding relatively well-defined PhBD–PBzMA diblock copolymers with dispersities of less than 1.20. A phase diagram was constructed to facilitate the reproducible targeting of spheres, worms and vesicles. At 25% w/w copolymer concentration, only kinetically-trapped spheres could be obtained when targeting core-forming PBzMA DPs of 30–300. Remarkably high copolymer concentrations (≥40% w/w) were required to access pure worms and vesicles for this particular PISA formulation. Finally, the physical properties of $PhBD_{80}$–$PBzMA_{40}$ worms were characterized by oscillatory rheology. It was determined that the worms formed free-standing gels above a critical gelation concentration of 5% w/w.

Conflicts of interest

There are no conflicts to declare.

Acknowledgements

S. P. A. acknowledges EPSRC for a four-year *Established Career* Particle Technology Fellowship (EP/R003009), which provided post-doctoral support for M. J. R. We thank Kraton Polymers LLC (Houston, USA) for the kind gift of the monohydroxy-capped hydrogenated polybutadiene precursor used in this study.

References

1 Plastics Europe, *Plastics - the Facts 2019. An Analysis of the European Plastics Production, Demand and Waste Data*, Association of Plastics Manufacturers.
2 T. C. M. Chung, Functional Polyolefins for Energy Applications, *Macromolecules*, 2013, **46**, 6671–6698.
3 M. Szwarc, 'Living' Polymers, *Nature*, 1956, **178**, 1168–1169.
4 D. Baskaran and A. H. E. Muller, Anionic Vinyl Polymerization—50 Years after Michael Szwarc, *Prog. Polym. Sci.*, 2007, **32**, 173–219.
5 N. Hadjichristidis, M. Pitsikalis, S. Pispas and H. Iatrou, Polymers with Complex Architecture by Living Anionic Polymerization, *Chem. Rev.*, 2001, **101**, 3747–3792.
6 Y. Ren, T. P. Lodge and M. A. Hillmyer, Synthesis, Characterization, and Interaction Strengths of Difluorocarbene-Modified Polystyrene–Polyisoprene Block Copolymers, *Macromolecules*, 2000, **33**, 866–876.
7 R. P. Quirk and S. Corona-Galvan, Controlled Anionic Synthesis of Polyisoprene–Poly(2-Vinylpyridine) Diblock Copolymers in Hydrocarbon Solution, *Macromolecules*, 2001, **34**, 1192–1197.
8 D. A. Hajduk, P. E. Harper, S. M. Gruner, C. C. Honeker, G. Kim, L. J. Fetters and G. Kim, The Gyroid: A New Equilibrium Morphology in Weakly Segregated Diblock Copolymers, *Macromolecules*, 1994, **27**, 4063–4075.
9 M. A. Hillmyer and F. S. Bates, Synthesis and Characterization of Model Polyalkane–Poly(Ethylene Oxide) Block Copolymers, *Macromolecules*, 1996, **29**, 6994–7002.

10 J. Chiefari, Y. K. B. Chong, F. Ercole, J. Krstina, J. Jeffery, T. P. T. Le, R. T. A. Mayadunne, G. F. Meijs, C. L. Moad, G. Moad, *et al.*, Living Free-Radical Polymerization by Reversible Addition–Fragmentation Chain Transfer: The RAFT Process, *Macromolecules*, 1998, **31**, 5559–5562.

11 G. Moad, E. Rizzardo and S. H. Thang, Living Radical Polymerization by the RAFT Process, *Aust. J. Chem.*, 2005, **58**, 379–410.

12 G. Moad, E. Rizzardo and S. H. Thang, Radical Addition–Fragmentation Chemistry in Polymer Synthesis, *Polymer*, 2008, **49**, 1079–1131.

13 H. De Brouwer, M. A. J. Schellekens, B. Klumperman, M. J. Monteiro and A. L. German, Controlled Radical Copolymerization of Styrene and Maleic Anhydride and the Synthesis of Novel Polyolefin-Based Block Copolymers by Reversible Addition-Fragmentation Chain-Transfer (RAFT) Polymerization, *J. Polym. Sci., Part A: Polym. Chem.*, 2000, **38**, 3596–3603.

14 A. J. D. Magenau, N. Martinez-Castro and R. F. Storey, Site Transformation of Polyisobutylene Chain Ends into Functional RAFT Agents for Block Copolymer Synthesis, *Macromolecules*, 2009, **42**, 2353–2359.

15 Y.-Y. Won, H. T. Davis and F. S. Bates, Giant Wormlike Rubber Micelles, *Science*, 1999, **283**, 960–963.

16 S. Jain and F. S. Bates, On the Origins of Morphological Complexity in Block Copolymer Surfactants, *Science*, 2003, **300**, 460–464.

17 J. Liu, Z. J. Thompson, H. J. Sue, F. S. Bates, M. A. Hillmyer, M. Dettloff, G. Jacob, N. Verghese and H. Pham, Toughening of Epoxies with Block Copolymer Micelles of Wormlike Morphology, *Macromolecules*, 2010, **43**, 7238–7243.

18 L. Bronstein, E. Krämer, B. Berton, C. Burger, S. Förster and M. Antonietti, Successive Use of Amphiphilic Block Copolymers as Nanoreactors and Templates: Preparation of Porous Silica with Metal Nanoparticles, *Chem. Mater.*, 1999, **11**, 1402–1405.

19 H. Kukula, H. Schlaad, M. Antonietti and S. Förster, The Formation of Polymer Vesicles or "Peptosomes" by Polybutadiene-block-poly(l-glutamate)s in Dilute Aqueous Solution, *J. Am. Chem. Soc.*, 2002, **124**, 1658–1663.

20 S. L. Canning, G. N. Smith and S. P. Armes, A Critical Appraisal of RAFT-Mediated Polymerization-Induced Self-Assembly, *Macromolecules*, 2016, **49**, 1985–2001.

21 N. J. Warren and S. P. Armes, Polymerization-Induced Self-Assembly of Block Copolymer Nano-Objects via RAFT Aqueous Dispersion Polymerization, *J. Am. Chem. Soc.*, 2014, **136**, 10174–10185.

22 B. Charleux, G. Delaittre, J. Rieger and F. D'Agosto, Polymerization-Induced Self-Assembly: From Soluble Macromolecules to Block Copolymer Nano-Objects in One Step, *Macromolecules*, 2012, **45**, 6753–6765.

23 W.-M. Wan and C.-Y. Pan, One-Pot Synthesis of Polymeric Nanomaterials via RAFT Dispersion Polymerization Induced Self-Assembly and Re-Organization, *Polym. Chem.*, 2010, **1**, 1475–1484.

24 W.-M. Wan, C.-Y. Hong and C.-Y. Pan, One-Pot Synthesis of Nanomaterials via RAFT Polymerization Induced Self-Assembly and Morphology Transition, *Chem. Commun.*, 2009, **39**, 5883–5885.

25 S. Boissé, J. Rieger, K. Belal, A. Di-Cicco, P. Beaunier, M.-H. Li and B. Charleux, Amphiphilic Block Copolymer Nano-Fibers via RAFT-Mediated Polymerization in Aqueous Dispersed System, *Chem. Commun.*, 2010, **46**, 1950–1952.

26 Y. Li and S. P. Armes, RAFT Synthesis of Sterically Stabilized Methacrylic Nanolatexes and Vesicles by Aqueous Dispersion Polymerization, *Angew. Chem., Int. Ed.*, 2010, **49**, 4042–4046.

27 S. Sugihara, A. Blanazs, S. P. Armes, A. J. Ryan and A. L. Lewis, Aqueous Dispersion Polymerization: A New Paradigm for in Situ Block Copolymer Self-Assembly in Concentrated Solution, *J. Am. Chem. Soc.*, 2011, **133**, 15707–15713.

28 X. Zhang, S. Boissé, W. Zhang, P. Beaunier, F. D'Agosto, J. Rieger and B. Charleux, Well-Defined Amphiphilic Block Copolymers and Nano-Objects Formed in Situ via RAFT-Mediated Aqueous Emulsion Polymerization, *Macromolecules*, 2011, **44**, 4149–4158.

29 L. Houillot, C. Bui, M. Save, B. Charleux, C. Farcet, C. Moire, J. A. Raust and I. Rodriguez, Synthesis of Well-Defined Polyacrylate Particle Dispersions in Organic Medium Using Simultaneous RAFT Polymerization and Self-Assembly of Block Copolymers. A Strong Influence of the Selected Thiocarbonylthio Chain Transfer Agent, *Macromolecules*, 2007, **40**, 6500–6509.

30 L. Houillot, C. Bui, C. Farcet, C. Moire, J. A. Raust, H. Pasch, M. Save and B. Charleux, Dispersion Polymerization of Methyl Acrylate in Nonpolar Solvent Stabilized by Block Copolymers Formed in Situ via the RAFT Process, *ACS Appl. Mater. Interfaces*, 2010, **2**, 434–442.

31 I. Chaduc, A. Crepet, O. Boyron, B. Charleux, F. D'Agosto and M. Lansalot, Effect of the pH on the Raft Polymerization of Acrylic Acid in Water. Application to the Synthesis of Poly(Acrylic Acid)-Stabilized Polystyrene Particles by RAFT Emulsion Polymerization, *Macromolecules*, 2013, **46**, 6013–6023.

32 W. Zhou, Q. Qu, Y. Xu and Z. An, Aqueous Polymerization-Induced Self-Assembly for the Synthesis of Ketone-Functionalized Nano-Objects with Low Polydispersity, *ACS Macro Lett.*, 2015, **4**, 495–499.

33 S. J. Byard, M. Williams, B. E. McKenzie, A. Blanazs and S. P. Armes, Preparation and Cross-Linking of All-Acrylamide Diblock Copolymer Nano-Objects via Polymerization-Induced Self-Assembly in Aqueous Solution, *Macromolecules*, 2017, **50**, 1482–1493.

34 J. Lesage de la Haye, X. Zhang, I. Chaduc, F. Brunel, M. Lansalot and F. D'Agosto, The Effect of Hydrophile Topology in RAFT-Mediated Polymerization-Induced Self-Assembly, *Angew. Chem., Int. Ed.*, 2016, **55**, 3739–3743.

35 W. J. Zhang, C. Y. Hong and C. Y. Pan, Fabrication of Spaced Concentric Vesicles and Polymerizations in RAFT Dispersion Polymerization, *Macromolecules*, 2014, **47**, 1664–1671.

36 E. R. Jones, M. Semsarilar, A. Blanazs and S. P. Armes, Efficient Synthesis of Amine-Functional Diblock Copolymer Nanoparticles via RAFT Dispersion Polymerization of Benzyl Methacrylate in Alcoholic Media, *Macromolecules*, 2012, **45**, 5091–5098.

37 L. A. Fielding, M. J. Derry, V. Ladmiral, J. Rosselgong, A. M. Rodrigues, L. P. D. Ratcliffe, S. Sugihara and S. P. Armes, RAFT Dispersion Polymerization in Non-Polar Solvents: Facile Production of Block Copolymer Spheres, Worms and Vesicles in n-Alkanes, *Chem. Sci.*, 2013, **4**, 2081–2087.

38 Y. Pei, J. M. Noy, P. J. Roth and A. B. Lowe, Soft Matter Nanoparticles with Reactive Coronal Pentafluorophenyl Methacrylate Residues via Non-Polar RAFT Dispersion Polymerization and Polymerization-Induced Self-Assembly, *J. Polym. Sci., Part A: Polym. Chem.*, 2015, **53**, 2326–2335.

39 M. J. Derry, L. A. Fielding and S. P. Armes, Industrially-Relevant Polymerization-Induced Self-Assembly Formulations in Non-Polar Solvents: RAFT Dispersion Polymerization of Benzyl Methacrylate, *Polym. Chem.*, 2015, **6**, 3054–3062.

40 Y. Pei, O. R. Sugita, L. Thurairajah and A. B. Lowe, Synthesis of Poly(Stearyl Methacrylate-b-3-Phenylpropyl Methacrylate) Nanoparticles in n-Octane and Associated Thermoreversible Polymorphism, *RSC Adv.*, 2015, **5**, 17636–17646.

41 M. J. Rymaruk, S. J. Hunter, C. T. O'Brien, S. L. Brown, C. N. Williams and S. P. Armes, RAFT Dispersion Polymerization in Silicone Oil, *Macromolecules*, 2019, **52**, 2822–2832.

42 M. J. Rymaruk, C. T. O'Brien, S. L. Brown, C. N. Williams and S. P. Armes, RAFT Dispersion Polymerization of Benzyl Methacrylate in Silicone Oil Using a Silicone-Based Methacrylic Stabilizer Provides Convenient Access to Spheres, Worms, and Vesicles, *Macromolecules*, 2020, **53**, 1785–1794.

43 Y. Kang, A. Pitto-Barry, H. Willcock, W.-D. Quan, N. Kirby, A. M. Sanchez and R. K. O'Reilly, Exploiting Nucleobase-Containing Materials – from Monomers to Complex Morphologies Using RAFT Dispersion Polymerization, *Polym. Chem.*, 2015, **6**, 106–117.

44 M. Zong, K. J. Thurecht and S. M. Howdle, Dispersion Polymerisation in Supercritical CO2 Using Macro-RAFT Agents, *Chem. Commun.*, 2008, **45**, 5942–5944.

45 Q. Zhang and S. Zhu, Ionic Liquids: Versatile Media for Preparation of Vesicles from Polymerization-Induced Self-Assembly, *ACS Macro Lett.*, 2015, **4**, 755–758.

46 J. Wang, M. Cao, P. Zhou and G. Wang, Exploration of a Living Anionic Polymerization Mechanism into Polymerization-Induced Self-Assembly and Site-Specific Stabilization of the Formed Nano-Objects, *Macromolecules*, 2020, **53**, 3157–3165.

47 C. Zhou, J. Wang, P. Zhou and G. Wang, A Polymerization-Induced Self-Assembly Process for All-Styrenic Nano-Objects Using the Living Anionic Polymerization Mechanism, *Polym. Chem.*, 2020, **11**, 2635–2639.

48 G. Moad, E. Rizzardo and S. H. Thang, Living Radical Polymerization by the RAFT Process-A Second Update, *Aust. J. Chem.*, 2009, **62**, 1402–1472.

49 R. C. Bening and C. L. Willis, Protected Functional Initiators for Making Terminally Functionalized Polymers, US005391663A, 1995.

50 K. Skrabania, A. Miasnikova, A. M. Bivigou-Koumba, D. Zehm and A. Laschewsky, Examining the UV-Vis Absorption of RAFT Chain Transfer Agents and Their Use for Polymer Analysis, *Polym. Chem.*, 2011, **2**, 2074–2083.

51 N. J. Warren, O. O. Mykhaylyk, D. Mahmood, A. J. Ryan and S. P. Armes, RAFT Aqueous Dispersion Polymerization Yields Poly(Ethylene Glycol)-Based Diblock Copolymer Nano-Objects with Predictable Single Phase Morphologies, *J. Am. Chem. Soc.*, 2014, **136**, 1023–1033.

52 J. Tan, C. Huang, D. Liu, X. Zhang, Y. Bai and L. Zhang, Alcoholic Photoinitiated Polymerization-Induced Self-Assembly (Photo-PISA): A Fast Route toward Poly(Isobornyl Acrylate)-Based Diblock Copolymer Nano-Objects, *ACS Macro Lett.*, 2016, **5**, 894–899.

53 A. P. Lopez-Oliva, N. J. Warren, A. Rajkumar, O. O. Mykhaylyk, M. J. Derry, K. E. B. Doncom, M. J. Rymaruk and S. P. Armes, Polydimethylsiloxane-Based Diblock Copolymer Nano-Objects Prepared in Nonpolar Media via RAFT-Mediated Polymerization-Induced Self-Assembly, *Macromolecules*, 2015, **48**, 3547–3555.

54 A. Blanazs, J. Madsen, G. Battaglia, A. J. Ryan and S. P. Armes, Mechanistic Insights for Block Copolymer Morphologies: How Do Worms Form Vesicles?, *J. Am. Chem. Soc.*, 2011, **133**, 16581–16587.

55 S. Perrier, 50th Anniversary Perspective: RAFT Polymerization - A User Guide, *Macromolecules*, 2017, **50**, 7433–7447.

56 L. A. Fielding, J. A. Lane, M. J. Derry, O. O. Mykhaylyk and S. P. Armes, Thermo-Responsive Diblock Copolymer Worm Gels in Non-Polar Solvents, *J. Am. Chem. Soc.*, 2014, **136**, 5790–5798.